Available online at www.sciencedirect.com
ScienceDirect
International Journal of Thermal Sciences 47 (2008) 175–181
International Journal of Thermal Sciences
www.elsevier.com/locate/ijts

Experimental studies on R134a-DMAC hot water based vapour absorption refrigeration systems

V. Muthu *, R. Saravanan, S. Renganarayanan

Institute for Energy Studies, Anna University, Chennai 600 025, India

Received 4 July 2006; received in revised form 14 February 2007; accepted 14 February 2007

Available online 2 April 2007

Abstract

The objective of this paper is to present an experimental study on environment friendly vapour absorption refrigeration system of 1 kW capacity using R134a-DMAC as the working fluids. The system is designed and tested for various operating conditions using hot water as heat source. In this paper, performance of the fabricated system are outlined with respect to various operating parameters such as heat source, condenser, absorber and evaporator temperatures. The result indicates that at the sink and source temperatures of 30 and 80 °C respectively and a typical heat input of 4 kW, the system attained steady state in two hours. For this system an actual COP of 0.25 to 0.45 was obtained under the tested conditions. The study reveals the feasibility of using R134a-DMAC as working fluids in the absorption machines using low potential heat sources for various applications.

Keywords: Absorption systems; Low temperature heat sources; Environment friendly working fluids; R134a-DMAC; COP

1. Introduction

The world demand of energy for the air-conditioning and refrigeration is increasing. This is due to an increasing desire for comfort, necessity of food storage and medical applications in hot climates especially third world developing countries.

The normal conventional cooling unit used for the above purpose is an electrically powered vapour compression machine, which often uses halogenized hydrocarbons (CFCs) as refrigerant with suitable substitute (HCFC). The Montreal Protocol marked a turning point in refrigeration industry and has a focus on international commitment to end the use of CFC and HCFC refrigerants aimed to protect the environment. One of the alternatives to overcome these draw-backs is vapour absorption refrigeration systems which use non-CFC/HCFC working fluids.

Absorption systems, being principally heat operated can utilize low potential heat sources like waste heat, solar energy, low-pressure steam etc. For large capacity systems, absorption systems consume very little high-grade electrical/mechanical energy compared to the vapour compression refrigeration system. Thus the absorption system can significantly contribute to the improvements in energy consumption efficiencies and also to energy conservation. The most commonly used refrigerant and absorbents pairs for VARS are water–lithium bromide and ammonia water. Some of the limitations encountered with these pairs are:

(1) Since water is used as refrigerant, evaporator temperature is limited to 5 °C and the system has to be operated under extremely low pressures (vacuum). There is also a possibility of lithium bromide salt crystallization at elevated temperatures and higher concentration, which will upset the operating parameters due to concentration variations;
(2) Ammonia–water system is toxic, rectification is necessary and copper cannot be used due to corrosion problem; and
(3) Ammonia with air is flammable when its concentration is about 25% by volume.

Because of these problems, in recent years considerable attention has been shifted to new working fluids for VARS. Among them many HFC/HCFC based working fluids have been

* Corresponding author. Tel.: Office +91 44 22203156, fax: +91 44 22353637.
E-mail address: vel_muthu@hotmail.com (V. Muthu).

1290-0729/$ – see front matter
doi:10.1016/j.ijthermalsci.2007.02.004

Nomenclature

COP	Coefficient of performance
COP_{car}	Carnot coefficient of performance
CR	Circulation ratio
E	Effectiveness or efficiency
m	Mass flow rate ..... kg/s
P	Pressure ..... bar
Q	Heat transfer rate ..... kW
t	Temperature ..... °C
X	Weight fraction of R134a in solution .... kg r/kg s
ε	Second law efficiency

Subscripts

a	Absorber or absorbent
act	Actual
c	Condenser or condensation or cooling
cw	Cooling water
e	Evaporator or evaporation
g	Generator
r	Refrigerant
rw	Chilled water
sink	Heat rejection sink
th	Thermodynamic
ws	Weak solution
1–18	State paints in the system with reference to Fig. 1.

Abbreviations

CFC	Chloro-fluoro-carbon
DMAC	*N*,*N*-dimethyl acetamide
R134a	1,1,1,2-tetrafluoroethane
VARS	Vapour absorption refrigeration system

identified [1–3]. Another major advantage of these systems is its capability to operate at moderate generator temperature, which makes these systems suitable for utilization of low potential heat sources such as waste heat/solar energy.

The search for new working fluids has centered on the halohydrocarbon group of fluids commercially known as Freons as the volatile component. These fluids meet most of the requirements for the desirable refrigerant. However, in comparison to ammonia and water, these fluids have a considerable lower enthalpy of vaporization. Number of investigators have considered and reported data for R134a as refrigerant with different absorbents for VARS [4–6]. It was experimentally found that Dimethyl Acetamide (DMAC) was found to be a very promising solvent for HCFC22 in VARS applications, and felt that the performance of HCFC134a-DMAC solution in VARS should be investigated [7]. Hence this study is focused on the experimental investigations on R134a-DMAC based absorption refrigeration systems.

2. Experimental set-up

The schematic diagram of the experimental set-up of the single stage continuous vapour absorption refrigeration system designed for 1 kW cooling capacity is shown in Fig. 1. Thermodynamic process cycle analysis have been carried out to estimate the heat interactions at the major components such as generator, condenser, evaporator, absorber and solution heat exchanger. These components are designed as per heat and mass transfer calculations using the standard design procedure.

The VARS employs an absorber, evaporator, condenser, generator, solution heat exchanger, solution pump, expansion valves and the piping to connect these. Heat is supplied to the generator from the heat source simulator. High-pressure refrigerant vapour, which is separated from the strong solution in the generator, enters to the condenser. Superheat and heat of condensation of refrigerant vapour are released to the cooling water flowing through condenser. Thus, the refrigerant vapour gets condensed and collected into the refrigerant receiver. Liquid refrigerant now passes via filter-drier, refrigerant flow meter and an expansion valve or capillary tube to the evaporator where it gets evaporated at a lower temperature absorbing heat from the refrigeration load simulator. A filter-drier is placed in the liquid line of refrigerant to remove moisture that may be present in the liquid R134a. The refrigerant vapour leaving the evaporator enters the bottom of the absorber where it is absorbed by the weak solution. Heat released during the absorption process and also during the mixing process is being rejected to the cooling water circuit. The solution now becomes strong in absorbent enters the strong solution reservoir. The solution pump enables its entry into the generator through the solution heat exchanger increases the pressure level of this solution. The strong solution-entering generator at the top of the shell is heated by circulated hot water and the refrigerant in the solution is separated. Hence, the solution becomes weak at high pressure and temperature. This solution enters the solution heat exchanger before entering the absorber for the improvement of system performance.

The various quantities to be measured during the course of experimentation are pressure, temperature, flow rate and heat interaction at all the major components at various locations as mentioned in Fig. 1. The various temperatures are to be measured are temperatures of refrigerant and absorbent Solution at various state points in the system and temperature of cooling water and ambient. Temperatures are measured using copper-constant an thermocouples (30 gauge). The uncertainty in the measurement of temperature was found to be ±0.5 °C. Since only positive pressures are encountered in the system, bourdon type pressure gauges are used for measuring these positive pressures at 10 locations in the circuit of the vapour absorption refrigeration system. The uncertainty in the pressure measurement is ±3.27%. Flow meters are used to monitor the flow rates of the liquid refrigerant and the strong solution. Hot water and cooling water flow rates are measured using water flow meter. The uncertainties for the refrigerant, solution and water flow measurement are ±6, ±2.9 and ±8.7% respectively.

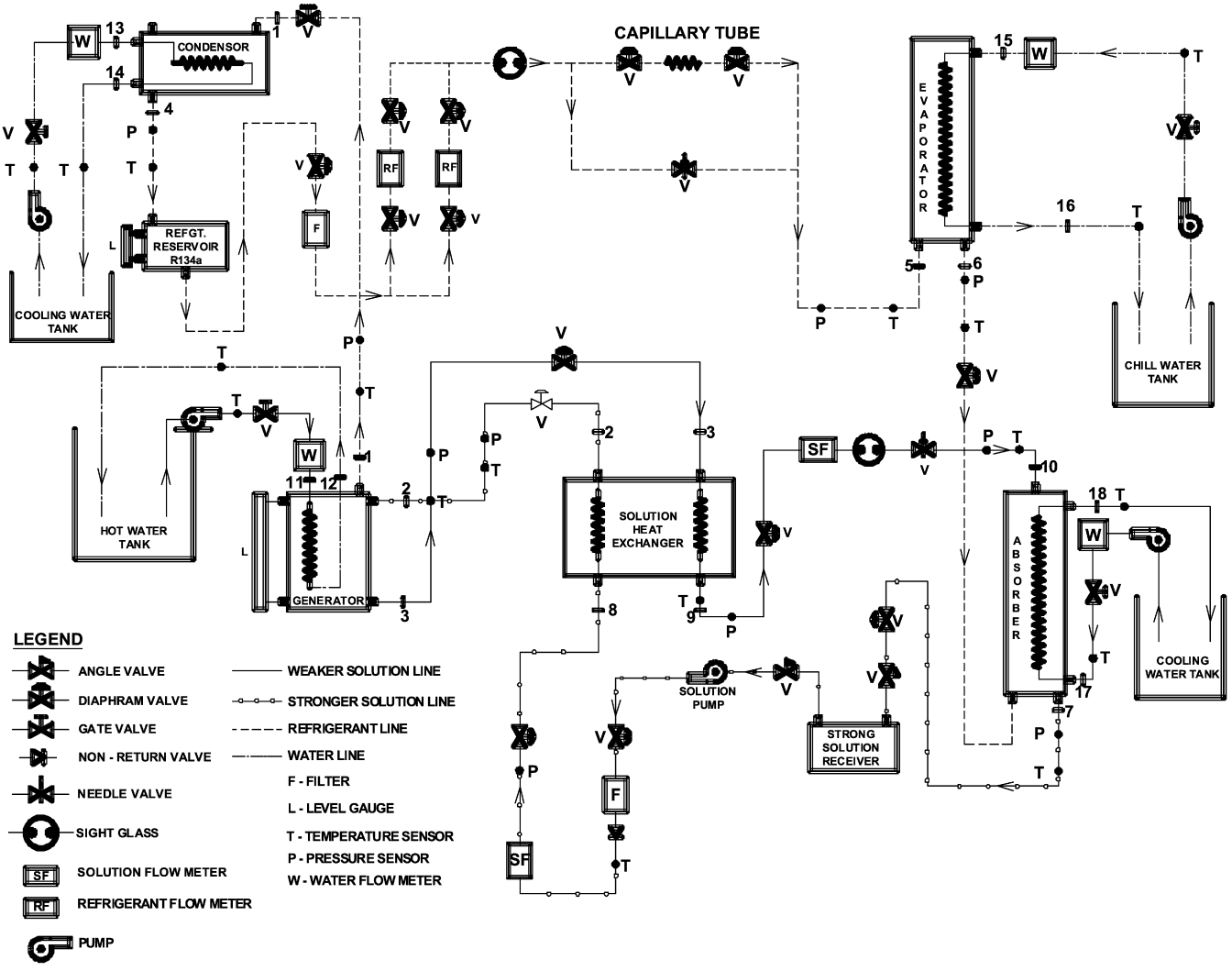

Fig. 1. Schematic diagram of experimental set-up.

3. Results and discussion

Experiments are carried out with R134a-DMAC as working fluid in the Single Stage Vapor Absorption Refrigeration System. The following ranges of operating conditions are fixed for testing the fabricated experimental setup.

(a) Temperatures of 60 and 80 °C were used to represent low potential heat energy sources. Higher temperature was not attempted, as the heat transfer fluid was water at atmospheric pressure.
(b) Cooling water temperatures (sink temperatures) were varied in the range of 20, 25 and 30 °C which covered for the typical ambient conditions.
(c) Evaporator temperature from about −5 to 15 °C aimed. This range is considered to cover a variation of variety of refrigeration requirements.

Heat quantities calculated from the measured temperature, pressure, mass flow rates and estimated concentration at steady state condition of the working fluids are designated as "thermodynamic values". The relevant equations are as given below: The state points are corresponding to the points represented in Fig. 1.

3.1. Thermodynamic heat quantities

Heat supplied at evaporator:

$$Q_{e,th} = m_r(h_6 - h_5) \tag{1}$$

Heat rejected at the condenser:

$$Q_{c,th} = m_r(h_1 - h_4) \tag{2}$$

Heat rejected at absorber:

$$Q_{a,th} = m_r h_6 + m_{ws} h_{10} - m_{ss} h_7 \tag{3}$$

Generator heat input:

$$Q_{g,th} = m_r h_1 + m_{ws} h_3 - m_{ss} h_2 \tag{4}$$

Recovered heat in solution heat exchanger:

$$Q_{h,th} = m_{ss}(h_2 - h_8) \tag{5}$$

"Actual" heat quantities are determined based on the measured flow rate and temperature rise (or drop) of water passing through each component.

3.2. Actual heat quantities

Heat rejected at absorber:

$$Q_{a,act} = m_{cw} cp_{cw} (T_{18} - T_{17}) \quad (6)$$

Generator heat input:

$$Q_{g,act} = m_{hs} cp_{hs} (T_{11} - T_{12}) \quad (7)$$

Heat supplied at evaporator:

$$Q_{e,act} = m_{rw} cp_{rw} (T_{15} - T_{16}) \quad (8)$$

Heat rejected at the condenser:

$$Q_{c,act} = m_{cw} cp_{cw} (T_{14} - T_{13}) \quad (9)$$

Where the specific heat capacities are calculated at the average temperature of water through each component.

From the above thermodynamic and actual heat quantities, the performance of each component is represented by its heat transfer effectiveness as follows:

Absorber:

$$E_a = Q_{a,act}/Q_{a,th} \quad (10)$$

Generator:

$$E_g = Q_{g,th}/Q_{g,act} \quad (11)$$

Heat exchanger:

$$Eh = (T_2 - T_8)/(T_3 - T_8) \quad (12)$$

Two important performance characteristics of VARS are, circulation ratio (CR) and coefficient of performance (COP).

CR is defined as the ratio of the mass flow of the strong solution to that refrigerant, i.e.

$$CR = m_{ss}/m_r \quad (13)$$

Coefficient of performance (COP) is defined as the ratio of the cooling load at evaporator (Q_e) to the heat energy input at generator (Q_g). Solution pump input being very small; has been neglected in the calculation of the COP. Therefore,

$$COP_{th} = Q_{e,th}/Q_{g,th} \quad (14)$$

Actual COP is calculated by means of actual heat supplied at generator and evaporator, i.e.

$$COP_{act} = Q_{e,act}/Q_{g,act} \quad (15)$$

Carnot Coefficient of Performance is given by the equation,

$$COP_{car} = \left(T_5/(T_4 - T_5) \times \left((T_3 - T_7)/T_3\right)\right) \quad (16)$$

Fig. 2 shows the variation of the temperature of the generator, absorber, condenser, and evaporator with respect to time. The plots are drawn for a constant heat source temperature 't_{hs}' of 80 °C and sink temperature of 30 °C. The mass flow rate of cooling water 'm_{cw}' is also held constant at around 0.33 kg/s, the generator temperature is seen to increase initially and then

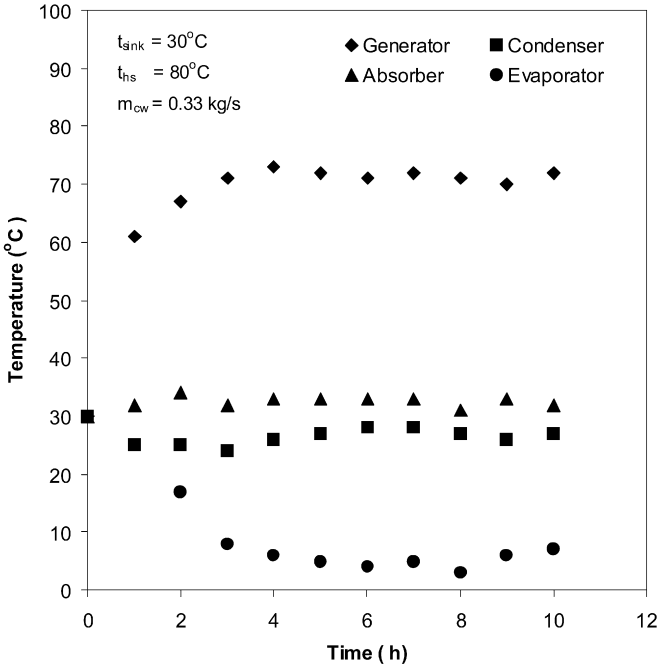

Fig. 2. Variation of component temperature with respect to time for constant sink and source temperatures.

after 3 hours it stabilizes at a temperature of around 74 °C. The variation of absorber and condenser temperature with time also follows the same pattern as the generator. From the figure it can be noticed that the absorber temperature is nearly always higher than the temperature of the condenser. This is due to higher heat load in the absorber because of the large heat of formation of solution involved in the absorption process. The evaporator temperature tends to decrease with time. This is obviously due to the cooling effect of the refrigerant. As can be seen from the figure the evaporator temperature reaches a stable condition after 5 hours. As the system is a heat operated one there is a heat carrying capacity for all the components of the system, this increased load causes the observed delay in reaching a stable evaporator temperature.

The variation of component temperatures with heat source temperature at constant temperatures is shown in Fig. 3. The mass flow rate of cooling water 'm_{cw}' is also held constant. It is clear from the figures that the operating temperatures at all components increase with heat source temperature. This is because of an increase in temperatures of both weak solution and refrigerant vapor at the respective outlet of generator. When the temperature of the refrigerant vapor leaving the generator and entering the condenser increases, cooling water flow rate through the absorber and condenser being kept constant, the condenser pressure and hence condenser temperature increases. Due to the increase of weak solution temperature at the outlet of the generator, weak solution temperature at the inlet of the absorber increases and therefore strong solution temperature at absorber outlet also increases. This causes the evaporator pressure and evaporator temperature to increase.

The variation of Circulation Ratio (CR) with Heat source temperature at constant evaporator temperature is shown in

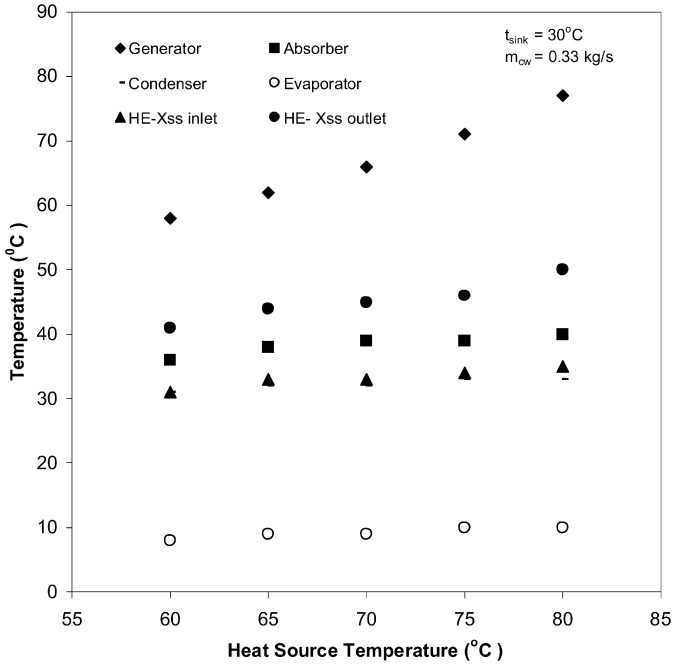

Fig. 3. Variation of component temperature with heat source temperature at steady state conditions.

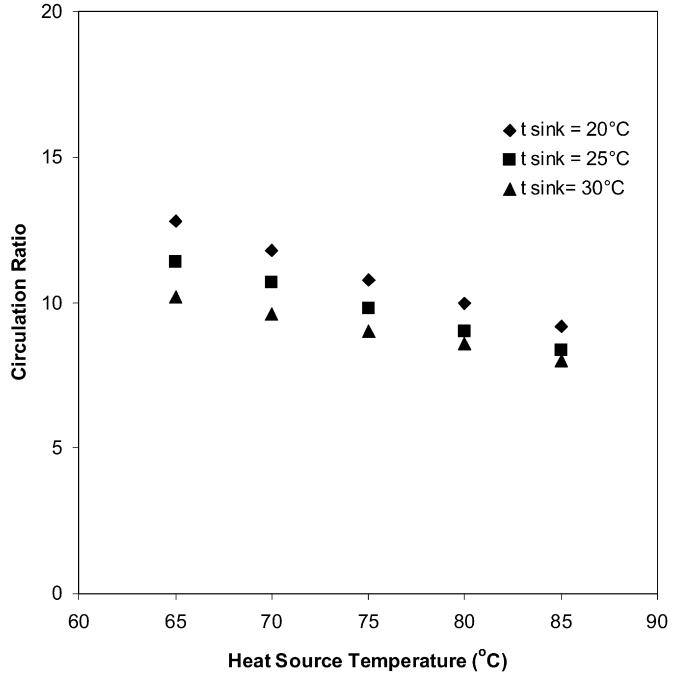

Fig. 4. Variation of circulation ratio with heat source temperature for different sink temperatures.

Fig. 4 for various sink temperatures. This can be attributed to the fact that the weak solution concentration decreases at a higher rate than that of strong solution when heat source temperature increases. Hence, when temperature and flow rate of cooling water are held constant, degassing width increases with heat source temperature, resulting in reduction of circulation ratio. As the sink temperature increases, the pressure of the heat source component increases, thereby increasing the heat source

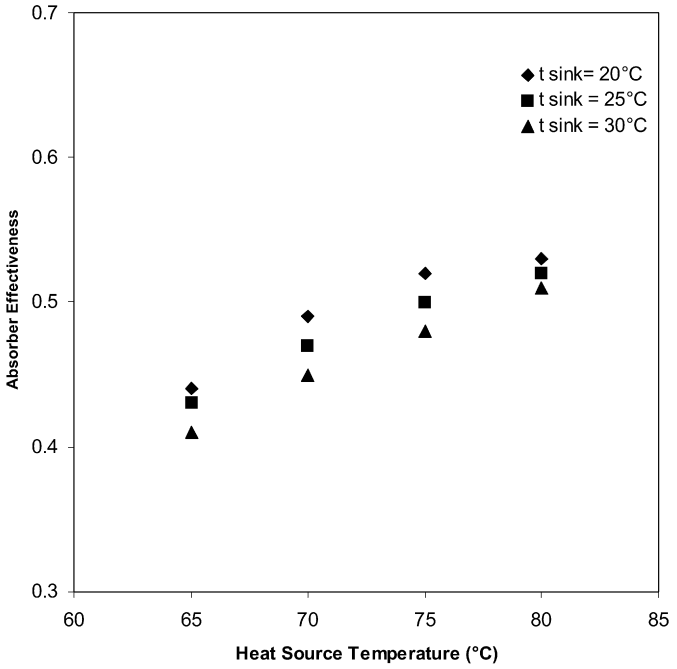

Fig. 5. Variation of absorber effectiveness with heat source temperature for different sink temperatures.

temperature. Thus, as explained above the circulation ratio decreases with increase in sink temperature.

The variation of absorber effectiveness with heat source temperature is shown in Fig. 5 for various sink temperatures at constant mass flow rate of cooling water. It is observed from the figure that as heat source temperature increases the effectiveness of the absorber is increasing, which is as expected. Now, since absorption is an exothermic process due to heat of mixing of solutions, it proceeds effectively at lower sink temperature. Therefore as sink temperature increases, the effectiveness of the absorber decreases. This can also be attributed to the fact that the increase of temperature of the weak solution in the absorber is not as much as the increase in sink temperature. Thus, the effectiveness of the absorber decreases with increase in sink temperature.

Fig. 6 shows the variation of both thermodynamic as well as actual cooling capacity as a function of heat source temperature at constant evaporator temperature 't_e' for various sink temperatures. It can be seen from the figure that cooling capacity increase with increase in heat source temperature. This is due to the increase in refrigerant flow rate at higher heat input to the generator. The rate of condensation and absorption is efficient at lower sink temperature. Hence there is an increase in cooling capacity at lower sink temperature. And it is also noticed from the figures that the thermodynamic quantities are more than the experimental values which is as expected.

The variation of both COP_a and COP_{th} with heat source temperature for constant evaporator temperature at 7 °C is shown in Fig. 7. It can be seen that the COP decreases as the heat source temperature increases. This is due to the large increase in the heat input at generator while the cooling load at evaporator is only slightly increased. It is also observed from the figure that

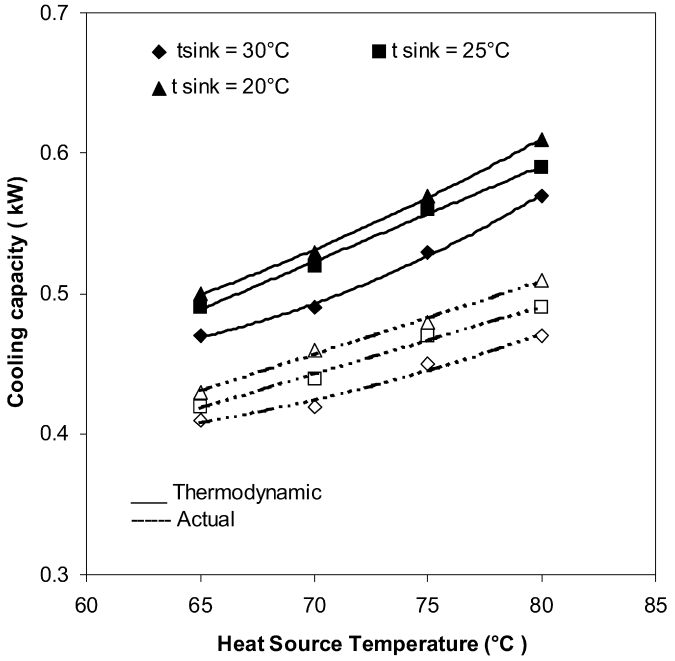

Fig. 6. Thermodynamic and actual cooling capacity variations with heat source temperatures for different sink temperatures.

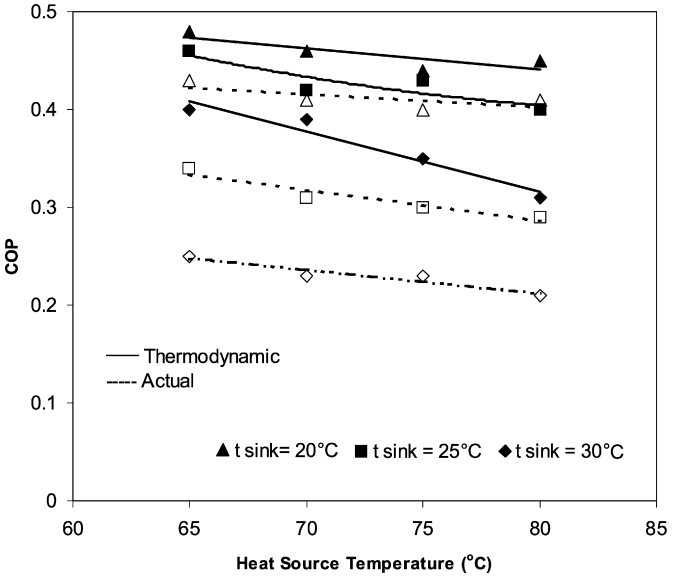

Fig. 7. Thermodynamic and actual COP variations with heat source temperatures for different sink temperatures.

the value of COP_{th} is higher than that of COP_a. This is obviously due to heat losses associated with experimental trials.

Fig. 8 shows the variation of COP with evaporator temperature at various sink temperatures. This variation is measured for a constant heat source temperature of 80 °C. The COP is seen to increase with increase in evaporator temperature. Now, at a nearly constant heat load at the generator, when the evaporator temperature increases there is a small increase in both refrigerant mass flow rate and cooling effect while the change of enthalpy at the inlet and outlet of the condenser is not significant. Thus with increase in cooling effect at nearly constant

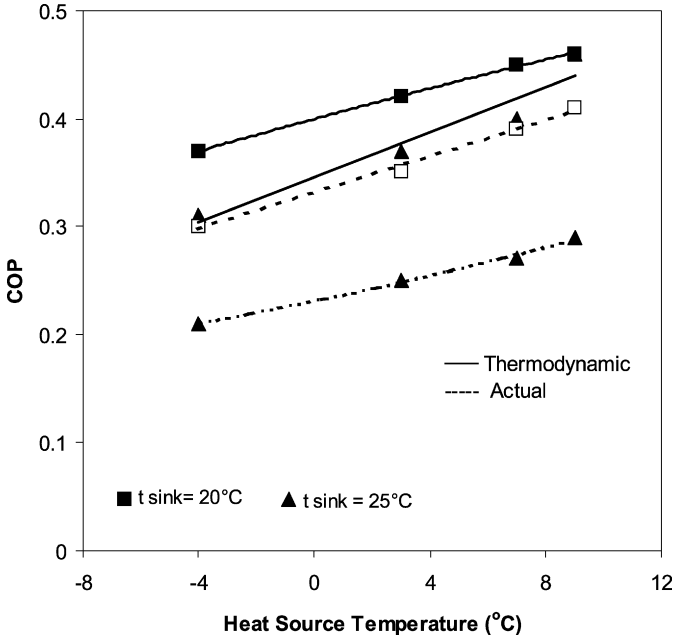

Fig. 8. Thermodynamic and actual COP variations with evaporator temperatures for different sink temperatures.

generator heat load the COP increases slightly. Again COP_a is less than the COP_{th} because of increase of actual heat input at generator. With increase in sink temperature the COP decreases. This is because the increase in sink temperature brings about increase in generator heat load. This increase causes a decrease of COP.

4. Conclusions

An experimental set up of 1 kW capacity is designed and fabricated using R134a-DMAC as working fluid and hot water as heat input. Experimental studies on the developed system are performed to evaluate the effects of various operating parameters on the systems performance. The specific conclusion arrived from these studies are listed as below:

(a) It is observed that sink temperature plays an important role in performance of the system.
(b) As the heat source temperature increases, heat quantities at generator, absorber, condenser and evaporator increase, while the circulation ratio decreases.
(c) Solution heat exchanger effectiveness, absorber effectiveness and generator effectiveness increase with increase in heat source temperature.
(d) At the sink and source temperatures of 20 and 80 °C respectively and a typical heat input of 4 kW, the system attained steady state in two hour. A steady evaporator temperature of about −4 °C is achieved.
(e) For the designed system and tested conditions an actual COP of 0.25 to 0.45 is attained.

The study reveals the feasibility of using R134a-DMAC as a working fluid in the future absorption machines using low potential heat sources.

Acknowledgements

Financial Support from the Science and Engineering Research Council (SERC), Department of Science and Technology, Government of India, New Delhi is gratefully acknowledged.

References

[1] B.J. Eiseman Jr., Why refrigerant 22 should be favoured for absorption refrigeration, ASHRAE J. (December 1959).
[2] M. Fatouh, S. Srinivasa Murthy, Comparison of R22-absorbent pairs for absorption cooling based on P-T-X data, Renewable Energy 3 (1993) 31–37.
[3] M. Fatouh, S. Srinivasa Murthy, Experimental studies on a R22-DMETEG absorption cooling system suitable for solar energy utilization, in: ISES Solar World Congress, Budapest, Hungary, 1993.
[4] A.C. Clelend, Polynomial curve-fits for refrigerant thermodynamic properties extension to include R134a, International Journal of Refrigeration 17 (4) (1994) 245–249.
[5] I. Borde, M. Jelinek, N.C. Daltrophe, Absorption system based on the refrigerant R134a, International Journal of Refrigeration 18 (6) (1995) 387–394.
[6] I. Borde, M. Jelinek, N.C. Daltrophe, Working fluids for an absorption system based on R124-chloro-1,1,1,2-tetrafluoroethane and organic absorbents, International Journal of Refrigeration 20 (4) (1997) 256–266.
[7] A.K. Songara, M. Fatouh, S. Srinivasa Murthy, Comparative performance of HFC 134a and HCF 22-based vapour absorption refrigeration systems, International Journal of Energy Research 21 (1997) 374–381.